Optical Receiver and Modulator Frequency Response Measurement with a Nd:YAG Ring Laser Heterodyne Technique

TUN S. TAN, MEMBER, IEEE, ROGER L. JUNGERMAN, MEMBER, IEEE, AND SCOTT S. ELLIOTT, SENIOR MEMBER, IEEE

Abstract—**The frequency response of optical receivers is accurately calibrated by measuring a heterodyne signal generated by mixing two Nd:YAG ring lasers. This heterodyne system offers more than 50 dB of dynamic range. Calibration of optical phase and amplitude modulators is achieved by down-converting a sideband of the modulated optical carrier to a fixed IF frequency with another laser. This technique eliminates the need for a high-speed receiver.**

I. Introduction

THE Nd:YAG ring laser [1], [2] is capable of generating a stable and narrow line width optical signal. By mixing the beams of two Nd:YAG ring lasers, a heterodyne signal at the beat frequency of the two lasers is generated. The wavelength of either laser can be controlled by varying the temperature of the YAG crystal. Thus, the frequency of the heterodyne signal can be swept over a wide range to accurately characterize the frequency response of an optical receiver. This dual YAG system is capable of generating the beat frequencies from dc to more than 100 GHz with better than 50 dB dynamic range.

The calibration of an optical amplitude modulator is often performed by direct measurement with a calibrated receiver. However, such a technique cannot measure the response of a phase modulator. In addition, as the bandwidth of the modulators increases it is important to develop techniques which do not depend on the availability of high-speed calibrated receivers. The technique we have developed uses two Nd:YAG lasers, one passing through the modulator, the other functioning as a local oscillator to convert one of the sidebands of the modulated carrier to a fixed IF frequency. This technique eliminates the need for a high-speed photoreceiver, has a good signal-to-noise ratio, and makes measurement of phase modulator frequency response possible.

II. Nd:YAG Ring Laser Heterodyne System

The laser used in this experiment is a diode laser pumped monolithic unidirectional ring oscillator which oscillates on the 1319 nm Nd:YAG transition [2]. It operates in a single mode with less than 3 kHz line width (Fig. 1) and a very stable frequency. These characteristics of this Nd:YAG ring laser make it an attractive optical source for precise calibration of the frequency response of optical devices. The schematic diagram for the calibration of photodiodes and optical receivers is shown in Fig. 2. The temperature of the Nd:YAG lasers and settings of the spectrum analyzer are controlled by a computer. The frequency versus temperature behavior of this YAG laser heterodyne system is characterized by fixing the temperature of one YAG while sweeping the temperature of the other. The beat frequency of the two YAG lasers is measured and plotted versus temperature in Fig. 3. There are mode hops which occur with approximately 12 GHz spacing, which are expected from the length of the optical path in the ring. For frequency sweeps of more than 12 GHz, more than one frequency versus temperature tuning band is used. The data from two or more bands are then pieced together to form a continuous sweep.

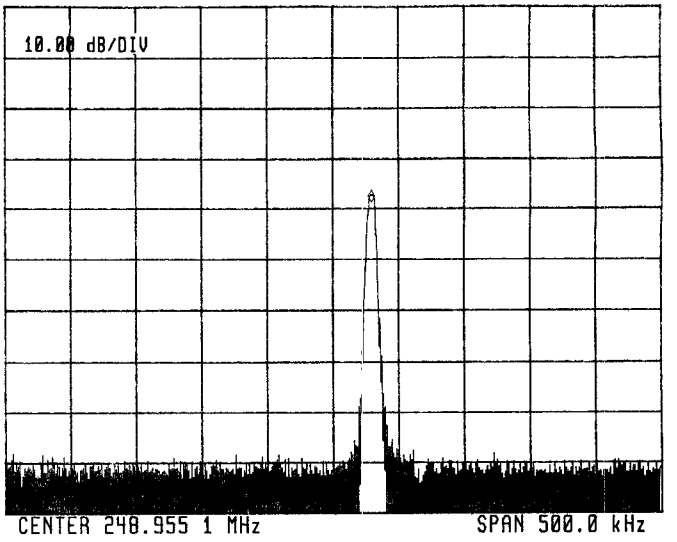

Fig. 1. Spectrum analyzer trace of heterodyne signal of two Nd:YAG ring lasers with line width less than 3 kHz FWHM.

III. Optical Receiver Calibration

The heterodyne signal is generated by combining the two YAG lasers with a polarization-preserving 3 dB coupler. The optical power (P_o) at the output of the coupler is

Manuscript received April 20, 1988; revised March 21, 1989.

The authors are with the Microwave Technology Division, Hewlett-Packard Company, 1412 Fountaingrove Parkway, Santa Rosa, CA 95401.

IEEE Log Number 8928846.

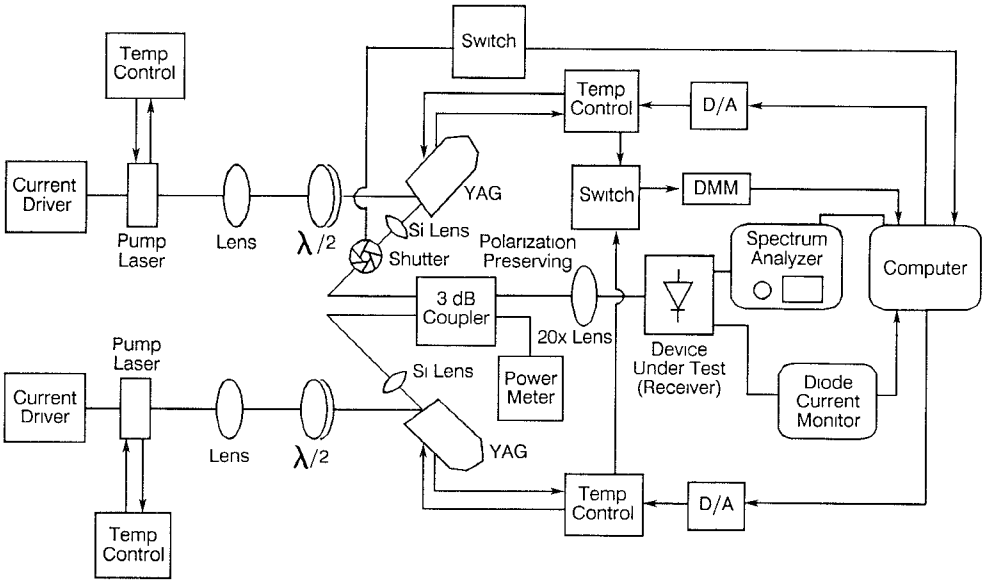

Fig. 2. Optical heterodyne measurement system for optical receivers.

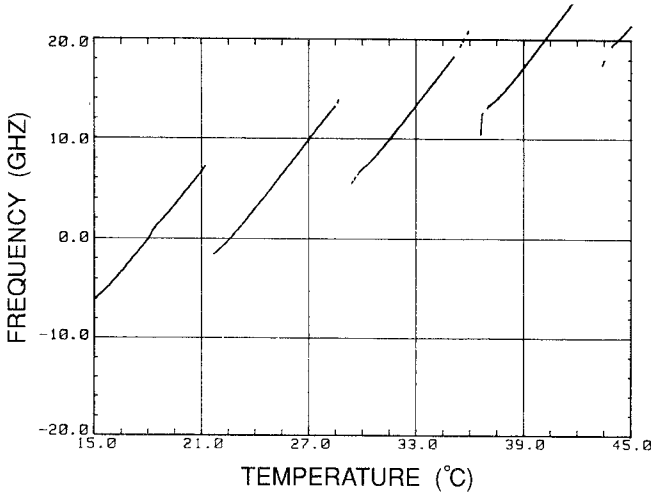

Fig. 3. Beat frequency versus YAG crystal temperature for the dual Nd·YAG ring laser heterodyne system.

of the form

$$P_o = P_{o1} + P_{o2} + 2\sqrt{P_{o1} \cdot P_{o2}} \cos(\omega_2 - \omega_1)t \qquad (1)$$

where P_{o1} and P_{o2} denote the optical power delivered to the receiver from the two YAG lasers. In (1) we assume that the mixing efficiency of the two lasers is 100 percent. This assumption is valid only if the lasers are linearly polarized and their polarizations are aligned along the same principal axis of the polarization-preserving fiber. A polarizer is inserted at the output of each laser to ensure that the lasers are linearly polarized. The polarization alignment of the lasers to the polarization-preserving fiber's axis is achieved using an iterative process involving a temperature modulation technique [3], with maximization of the extinction ratio and heterodyne signal.

The RF responsivity of a receiver is defined as

$$R = \frac{i_{\text{rms}}}{P_{\text{rms}}} \qquad (2)$$

where i_{rms} is the root-mean-square photocurrent and P_{rms}

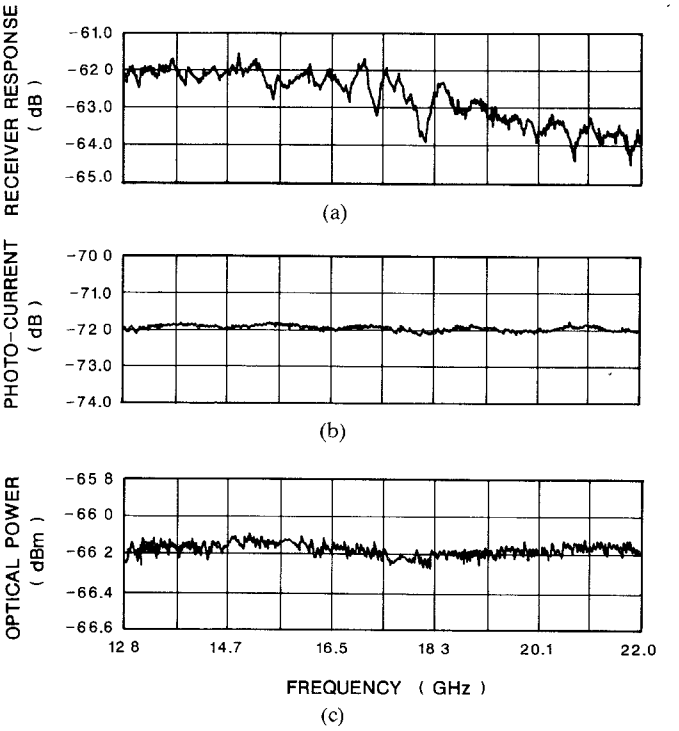

Fig 4. Measured responses of the optical receiver: (a) receiver frequency response, (b) photocurrent, and (c) input optical power.

is the root-mean-square optical power swing. The value of i_{rms} is obtained from the output of the microwave spectrum analyzer using the relationship $i_{\text{rms}} = \sqrt{P_s / Z_0}$, where P_s is the peak power detected at the spectrum analyzer and $Z_0 = 50\ \Omega$ is the impedance of the analyzer.

$$P_{\text{rms}} = \frac{1}{\sqrt{2}} \cdot 2\sqrt{P_{o1} \cdot P_{o2}}$$

$$= R_{\text{dc}} \cdot \sqrt{2 i_1 \cdot i_2} \qquad (3)$$

where i_1 and i_2 are the photocurrents from the receiver due to two lasers respectively and R_{dc} is the relationship

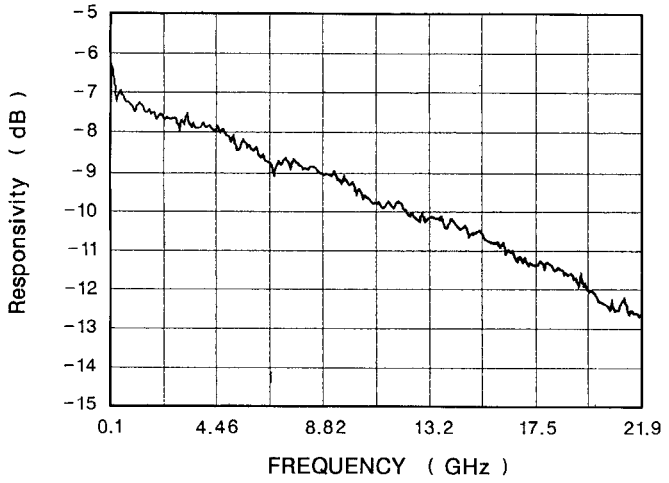

Fig. 5. The final calibrated frequency response of the optical receiver.

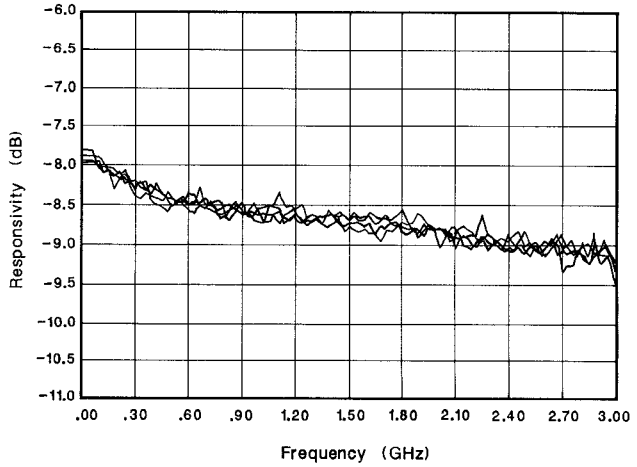

Fig. 6. Repeatability measurement of a 3 GHz receiver.

between the photocurrent of the receiver and the optical power delivered to the receiver, also known as the dc responsivity, which can be calibrated with an optical power meter and a current meter.

Equation (2) can be expressed in measurable quantities:

$$R = \frac{1}{R_{\mathrm{dc}}} \cdot \sqrt{\frac{P_s}{2Z_0 i_1 i_2}}. \tag{4}$$

In order to monitor the variation in the laser powers or photocurrents individually, a mechanical shutter is incorporated as shown in Fig. 2. Fig. 4(a) shows the uncalibrated frequency response of an optical receiver with an InP/InGaAs high-speed photodiode [4]. The photocurrent of the receiver and the input optical power from the YAG lasers are also measured, as shown in Fig. 4(b) and (c), and show less than 0.5 dB variation during the measurement. The final calibrated frequency response of the receiver is obtained by subtracting errors due to the cable, the spectrum analyzer, and the variation in optical power. The final calibrated responsivity versus frequency of the receiver is shown in Fig. 5. The repeatability of the measurement is better than ± 0.25 dB for the 22 GHz frequency

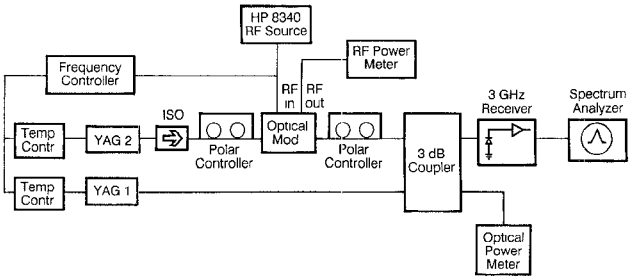

Fig. 7. Optical heterodyne measurement system for an optical modulator.

range. A 3 GHz receiver calibration (Fig. 6) shows repeatability of better than 0.3 dB since only a single temperature versus frequency tuning band is required.

IV. Optical Modulator Calibration

We have investigated the use of the dual-YAG heterodyne technique for the characterization of $LiNbO_3$ integrated optic modulators. Recently, optical modulators have been fabricated with response extending out to millimeter-wave frequencies [5], [6]. Directly measuring the response at these high frequencies presents difficulties in obtaining sufficiently fast photodiodes and in calibrating the optical receiver. Several techniques have been demonstrated for characterizing the frequency response of amplitude modulators using a low-frequency uncalibrated optical receiver [6]–[8]. The heterodyne method we describe here also employs a low-frequency receiver and makes it possible to measure both amplitude and phase modulators.

The heterodyne modulator calibration is shown in Fig. 7. Consider first measurements on a Mach–Zehnder interferometer intensity modulator [9] biased in quadrature (half-on) driven with a small RF modulation signal of frequency ω_m. The amplitude of the local oscillator laser measured at the detector is

$$L_R = A_1 e^{j\omega_1 t}. \tag{5}$$

For small-signal modulation, the amplitude of the optical signal through the modulator, measured at the photoreceiver, is

$$M_R = A_2\left(1 + M(\omega_m)\cos\omega_m t\right) e^{j\omega_2 t} \tag{6}$$

where $M(\omega_m)$ is the modulation index produced by the Mach–Zehnder interferometer ($M(\omega_m) \ll 1$) and A_1 and A_2 are the magnitudes of the amplitudes of the local oscillator and modulator signals respectively, measured at the detector with no modulation signal applied. These two signals mix in the photodetector to give a detected photocurrent of

$$i_R = R(L_R + M_R)(L_R^* + M_R^*) \tag{7}$$

where R is the responsivity of the detector in A/W. Considering terms within the bandwidth of the photore-

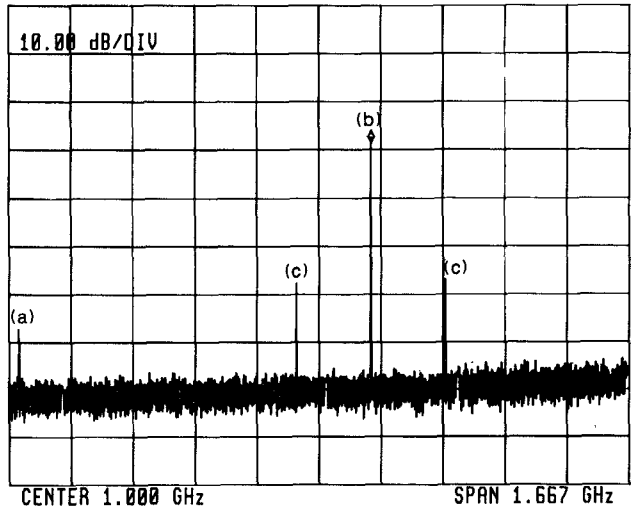

Fig. 8. Signals detected at the spectrum analyzer for the amplitude modulator measurement: (a) directly modulated signal; (b) heterodyne signal of two lasers; (c) sidebands of the carrier.

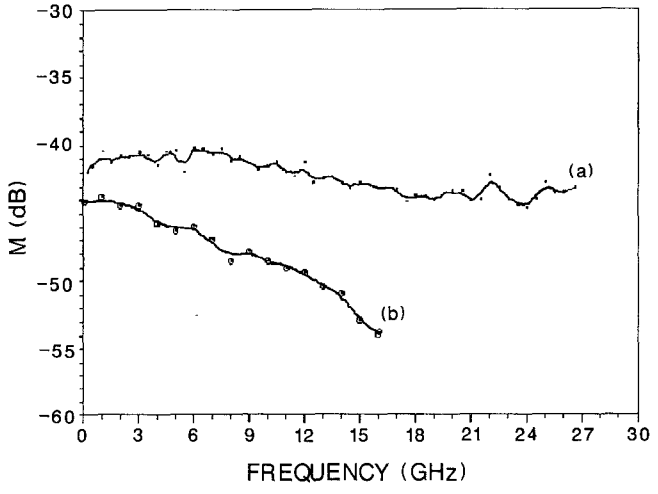

Fig. 9. Measured frequency response of amplitude modulators: (a) $\{+ + - +\}$ phase reversal electrode amplitude modulator; (b) uncoded device.

ceiver we find

$$i_R/R = A_1^2 + [A_2(1 + M(\omega_m)\cos\omega_m t)]^2 + A_1A_2(1+M(\omega_m)\cos\omega_m t)[e^{j(\omega_1-\omega_2)t}+e^{-j(\omega_1-\omega_2)t}]. \quad (8)$$

Since $M(\omega_m) \ll 1$, (8) reduces to

$$i_R/R = A_1^2 + A_2^2 + 2A_2^2(M(\omega_m)\cos\omega_m t) + 2A_1A_2\cos(\omega_1-\omega_2)t + M(\omega_m)A_1A_2[\cos(\omega_1-\omega_2-\omega_m)t + \cos(\omega_1-\omega_2+\omega_m)t]. \quad (9)$$

The term at frequency ω_m represents direct AM detection and varies linearly with the optical intensity through the modulator. The term at frequency $\omega_1-\omega_2$ is the heterodyne signal with upper and lower sidebands displaced by frequency ω_m. The heterodyne signals are proportional to the amplitude of the field through the modulator, A_2, which can be small due to insertion loss in the modulator. Thus, the heterodyne signals may be larger than the direct AM if a strong local oscillator laser signal, A_1, is used. Fig. 8 shows the signals displayed on a spectrum analyzer with $\omega_1-\omega_2 = 1.14$ GHz and $\omega_m = 200$ MHz. The heterodyne sideband is 10 dB larger that the directly detected signal. Fig. 9 shows the measured frequency response for a fiber pigtailed $\{+ + - - +\}$ phase reversal electrode amplitude modulator [5] to 26.5 GHz. The response of the uncoded modulator (without phase reversals) 1 cm in length is also plotted and shows the predicted high-frequency roll-off compared with the coded device.

We next consider the calibration of an optical phase modulator. For a phase-modulated signal, (6) becomes

$$M_R = A_2 e^{j[M(\omega_m)\sin\omega_m t+\omega_2 t]} \quad (10)$$

where $M(\omega_m)$ is now the modulation index of the optical phase modulator. Substituting into (7), the photocurrent

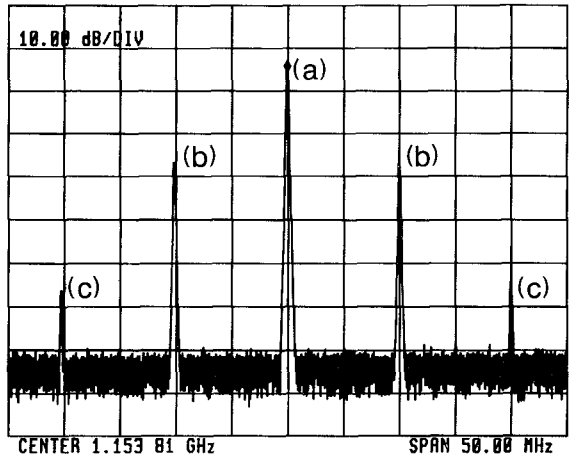

Fig. 10. Signal detected at the spectrum analyzer for the phase modulator: (a) heterodyne signal of two lasers; (b) fundamental sidebands of the carrier; (c) sidebands at the second harmonic.

produced by beating the phase-modulated signal with the local oscillator laser is

$$i_R/R = A_1^2 + A_2^2 + 2A_1A_2\cos(M(\omega_m)\sin\omega_m t + (\omega_1-\omega_2)t). \quad (11)$$

Expanding (10) in terms of Bessel functions,

$$i_R/R = A_1^2 + A_2^2 + 2A_1A_2[J_0(M(\omega_m))\cos(\omega_1-\omega_2)t + J_1(M(\omega_m))\cos(\omega_1-\omega_2+\omega_m)t - J_1(M(\omega_m))\cos(\omega_1-\omega_2-\omega_m)t + J_2(M(\omega_m))\cos(\omega_1-\omega_2+2\omega_m)t + \cdots]. \quad (12)$$

The heterodyne and first and second harmonic phase modulation sidebands are shown in Fig. 10 as displayed on a spectrum analyzer (for $\omega_1-\omega_2 = 1.15$ GHz and $\omega_m =$ 10 MHz). In Fig. 11 the variation of the heterodyne signal and the first and second harmonic sidebands is plotted as a function of drive level and compared with theory. Assuming a modulation efficiency of 0.14 rad/V, good agree-

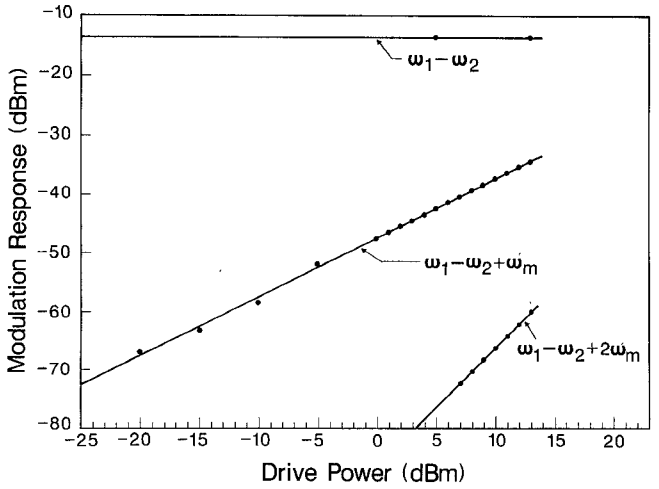

Fig. 11. Variation of optical phase modulator sidebands as a function of RF drive power to the modulator. Direct heterodyne $(\omega_1-\omega_2)$, fundamental sideband $(\omega_1-\omega_2+\omega_m)$, and second harmonic sideband $(\omega_1-\omega_2+2\omega_m)$ are shown.

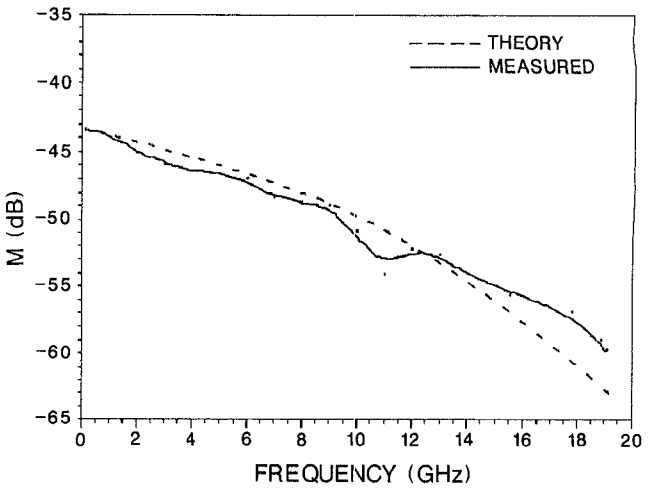

Fig. 12. Measured and calculated frequency responses of the phase modulator.

ment is obtained with the experimental data. This modulation efficiency is consistent with the measurement of a switching voltage of 5.5 V for Mach–Zehnder amplitude modulators with the same electrode pattern (1 cm long device). To evaluate the modulation efficiency from the switching voltage it is necessary to include the effect of the 28 Ω series resistor required to match to the 22 Ω electrode transmission line.

The presence of residual amplitude modulation in a phase modulator can be measured in two ways. Since $J_1(M[\omega_m]) = -J_{-1}(M[\omega_m])$, the upper and lower fundamental sidebands of the heterodyne signal in (12) are of opposite phase. However, for amplitude modulation the two sidebands are in phase. Thus, a combination of amplitude and phase modulation will be seen as unequal sideband heights if the magnitudes of each type of modulation are comparable. For a small amount of AM, the amplitude can be directly measured at frequency ω_m and the phase modulation measured by evaluating the heterodyne sidebands using (12). For the phase modulator described in Fig. 11, the direct AM signal was observed to be -67 dBm with 13 dBm drive to the modulator. The optical intensity through the modulator (A_2^2) was measured to be -15.5 dBm, and the local oscillator signal (A_1^2) was -10.4 dBm. From (9) and (12), the residual amplitude modulation is seen to be -29 dB below the phase modulation sideband at offset frequency ω_m. Thus, no significant difference between the upper and lower sideband power is expected. The amplitude modulation present in the $LiNbO_3$ phase modulator is probably explained by the absence of antireflection coatings on the end faces of the modulator. The 4 percent reflection between the epoxied pigtail and the modulator crystal at the input and output of the device is consistent with the observed level of residual amplitude modulation.

In Fig. 12, $M(\omega_m)$ is plotted as a function of frequency for a 1 cm uncoded phase modulator. $M(\omega_m)$ is measured by tracking one of the sidebands with the local oscillator laser, as was done for the measurement of the amplitude modulator. The measured response shows good agreement with the theoretical curve.

V. Conclusion

A dual Nd:YAG ring laser heterodyne system for the calibration of optical receivers has been demonstrated. Such a system can potentially be used as a calibration standard for optical receivers and photodiodes. This heterodyne system is also used to measure the response of both phase and amplitude modulators without the need for and precise calibration of a high-speed receiver, and provides an extended dynamic range in the measurements.

Acknowledgment

The authors would like to thank R. Trutna and D. Donald for their assistance in the construction of the YAG heterodyne system, P. Hernday and R. Van Tuyl for consultation in receiver calibration, and J. Ballantyne, R. Chavez, and D. Derrickson for the computer software program used in the measurements.

References

[1] T. J. Kane and R. L. Byer, "Monolithic, unidirectional single mode Nd:YAG ring laser," *Opt. Lett.*, vol. 10, pp. 65–67, Feb. 1985.

[2] W. R. Trutna, D. K. Donald and, M. Nazarathy, "Quasiplanar unidirectional ring laser," in *Conf. Lasers and Electro-Optics Dig.* (Washington DC), 1987 p. 188.

[3] G. R. Walker and N. G. Walker, "Alignment of polarisation-maintaining fibres by temperature modulation," *Electron. Lett.*, vol. 23, no. 13, June 1987.

[4] S. Y. Wang, K. W. Carey, and B. H. Kolner, "A front-side-illuminated InP/GaInAa/InP p-i-n photodiode with a −3-dB bandwidth in excess of 18 GHz," *IEEE Trans. Electron Devices*, vol. ED-34, pp. 938–940, Apr. 1987.

[5] R. L. Jungerman, D. W. Dolfi, M. Nazarathy, and C. A. Johnsen, "Coded phase reversal $LiNbO_3$ modulator with bandwidth greater than 20 GHz at 1.3 μm wavelength," *Electron. Lett.*, vol. 23, pp. 172–173, 1987.

[6] S. K. Korotky, G. Eisenstein, R. S. Tucker, J. J. Veselka, and G. Raybon, "Optical intensity modulation to 40 GHz using a waveguide electro-optic switch," *Appl. Phys. Lett.*, vol. 50, pp. 1631–1633, 1987.

[7] R. L. Jungerman, R. C. Bray, E. R. Ehlers, C. A. Johnsen, and T. S. Tan, "Two-tone measurements of optical modulator response," in *Opt. Commun. Conf. Dig.*, vol. 1 (Washington, D. C.), 1988, pp. 118.
[8] S. Uehara, "Calibration of optical modulator frequency response with application to signal level control," *Appl. Opt.*, vol. 17, pp. 68–71, 1978.
[9] R. C. Alferness, "Waveguide electrooptic modulators," *IEEE Trans. Microwave Theory Tech.*, vol. MTT-30, pp. 1121–1137, 1982.

Roger L. Jungerman (S'85–M'85) received the M.S. and Ph.D. degrees in applied physics from Stanford University, Stanford, CA, in 1983 and 1985 respectively. His dissertation involved optical measurements of surface acoustic waves and a phase-sensitive scanning optical microscope.

Since 1985, he has been at Hewlett-Packard, Santa Rosa, CA, working on the design, fabrication, and packaging of lithium niobate integrated optic devices.

Dr. Jungerman is a member of the Optical Society of America.

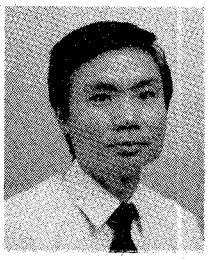

Tun S. Tan (S'70–M'77) received the B.S. degree in electrical engineering from the Massachusetts Institute of Technology in 1971 and the M.S. and Ph.D. degrees in electrical engineering from Stanford University, Stanford, CA, in 1973 and 1977, respectively.

In 1976, he joined Hewlett-Packard Company, Santa Rosa, CA, and has been involved in the design, modeling, fabrication, and application of GaAs devices. He was one of the developers of the first surface acoustic wave resonators used in microwave instruments. He led a team of engineers for the development of low-distortion *K*-band power GaAs FET's used in microwave and millimeter-wave test instruments and holds a patent on a submicron gate process. He has been a development engineer, a project leader, and a project manager. His current research interests are in photonic instruments, optoelectronic devices, and fiber-optic and coherent detection.

Dr. Tan is a member of Tau Beta Pi, Sigma Xi, and Eta Kappa Nu.

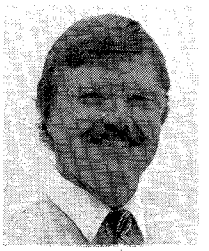

Scott S. Elliott (M'66–SM'83) received the B.S.E.E. and M.S.E.E. degrees from the University of California at Berkeley in 1969 and 1971, respectively. After working in the area of microwave ferrites for several years, he returned to school to receive the degree of Ph.D. in electrical engineering from the University of California at Santa Barbara in 1978.

He joined the Technical Staff at the Hewlett-Packard Microwave Technology Division in Santa Rosa, CA, in 1978, where he has worked as an MTS, a Project Manager, and R&D Section Manager, and currently as the Manufacturing Engineering Manager. His work has included the development of surface acoustic wave resonators and filters, millimeter-wave semiconductor devices, and high-speed optical devices for instrument applications. He is currently involved in the manufacture of gallium arsenide integrated circuits.